water

MDPI

Article

Sand Transport with Cohesive Admixtures. Laboratory Tests and Modeling

Jerzy Zawisza [1,*], Iwona Radosz [1], Jarosław Biegowski [2] and Leszek M. Kaczmarek [1]

[1] Faculty of Civil Engineering, Environmental and Geodetic Sciences, Koszalin University of Technology, 75-453 Koszalin, Poland
[2] Institute of Hydro-Engineering, Polish Academy of Sciences, 80-328 Gdańsk, Poland
* Correspondence: jerzy.zawisza@tu.koszalin.pl

Abstract: The paper presents results of experimental and theoretical studies on transport of water-sand mixtures in steady flow with small amounts of cohesive fractions. The experiments were carried out for sand alone and with cohesive admixtures in the form of clay in the amount of 5, 10, 15 and 20% by weight. The amount of sand fractions retained in the trap and along the control area was measured. The experimental results were compared with the calculation results for transport rate of sand fractions. An intended model of the vertical structure of both sand velocity and concentration as well as vertical mixing and sorting is proposed here in order to determine the influence of cohesive admixtures on the transport of sand fractions. Hence the reduction of sand fractions transport due to cohesion forces is included. The agreement of sand transport calculations according to the extended model with measured results and experimental data from literature was achieved within plus/minus a factor of 2.

Keywords: steady flow; sand transport; sediment mixture; cohesive admixture; grain size distribution

Citation: Zawisza, J.; Radosz, I.; Biegowski, J.; Kaczmarek, L.M. Sand Transport with Cohesive Admixtures. Laboratory Tests and Modeling. *Water* **2023**, *15*, 804. https://doi.org/10.3390/w15040804

Academic Editors: Sergey R. Chalov and Michal Habel

Received: 08 January 2023
Revised: 07 February 2023
Accepted: 16 February 2023
Published: 18 February 2023

1. Introduction

Sediment transport that takes place along river channels, at the bottom of bays, lagoons or rainwater or sanitary sewers for most substrates involves sediment, which is composed of non-cohesive fractions but there are also places where layers of sediment with various properties of sand and cohesive admixture combinations are deposited.

Substances of inorganic origin (dust, silt) and organic origin (microbenthos biota, dead organisms, their parts and also substances resulting from metabolism) can play the role of bonding admixtures. Determination of the transport of this type of sediment is an important problem not only due to the change in bathymetry, but also due to the transfer of biogenic substances and pollutants. The wide spectrum of substances introducing cohesion forces in the sediment is a major difficulty in modeling, as each substance has different physical and chemical properties.

Such mixtures contribute to many problems in the design, maintenance and management of waterways. The mechanism of sediment transport in open and closed channels is also a significantly important issue for the design of sanitary and storm sewers. The presence of sediment in sewer lines significantly affects the proper functioning of the system.

The history of scientific research on the dynamics of sandy sludge with the addition of bonding agents compared to studies of "pure" sands is much shorter. While the prediction of the transport velocity of non-cohesive sediments proposed by French engineer MP du Boys [1] dates back to the 19th century, the first theoretical attempts to describe the flocculation process started only in the early 20th century. Among the authors of the pioneering attempts are Smoluchowski [2], Camp and Stein [3] and Partheniades [4], in addition to subsequent researchers with significant contributions such as Migniot [5], Ives

[6], Winterwerp [7], Winterwerp and Kranenburg [8], Mc Anally and Mehta [9]. Tsai et al. [10] studied the effect of shear in aqueous mixtures with natural bottom sediments and suggested a dependence of the collision mechanism on particle size. Lick and Lick [11] present a general model of floc dynamics that includes the effects of disaggregation due to collision and shear. The starting point of Tsai and Hwang's [12] consideration was the assumption of a change in particle velocity due to collisions, aggregation and disintegration. In turn, Mc Anally and Mehta [9] developed a dynamic formula for aggregation of fine estuarine sediments.

Winterwerp [7] and Winterwerp and Kranenburg [8] developed the flocculation model by adopting fractal theory. The concept of fractal geometry has been widely used to describe flocculation geometry, and Winterwerp's model [7] describes one characteristic floc size and takes turbulence as the dominant factor affecting flocculation processes. This model assumes a constant value of fractal dimension, such as 2.0 and 2.2 (Winterwerp [7] and Winterwerp et al. [13]). Although the use of a constant fractal dimension is a simplification, it is of practical importance, although the application of this assumption to sediment transport in different regimes is questionable. For example, the fractal dimension of a floc in the water column of a dilute flow is considered to be about 2.0 (Hawley [14], Meakin [15]). However, based on the mixtures in estuaries observed during field studies, noticeable changes in the fractal dimension have been obtained (Dyer and Manning [16]). Using measured parameters and constitutive relationships in rheology (Kranenburg [17]), for effective stress in bed consolidation (Merckelbach and Kranenburg [18]) found that the resulting fractal dimension is much larger than 2.0 (about 2.75). Khelifa and Hill [19] presented the concept stating that in a consolidated deposit, in which the flock structure is completely destroyed, the fractal dimension is 3.0. Therefore, a general flocculation model, which is able to describe the dynamics of flocks starting from the lower boundary of the moving bottom and ending at the contact layer, must include a variable fractal dimension.

It has also been shown that an assessment of sediment flux can be the basis for determination of erosion rates (Boyer et al. [20]). The erosion flux E[kgm^{-2} s^{-1}] is quantified using the erosion threshold (Partheniades [4] and Winterwerp and van Kesteren [21]). Thresholds determine the proportion of shear stress τ [Nm^{-2}] of the flow relative to the critical stress that causes erosion of the eroded surface τ_{ce} [Nm^{-2}]. The above parameters are determined by experiments under laboratory conditions for sediment transport.

In case of non-cohesive sediments, research has defined the erosion threshold as a function of particle diameter d[m], as graphically presented in the diagrams of Hjulström [22] and Shields [23]. As determined by Migniot [5], the onset of erosion also depends on the angle of internal friction and the shape of particles. Probabilistic models using such parameters present good experimental consistency, as shown by Wiberg and Smith [24] and Dey [25]. It seems that correlations of this type prove to be a better fit for coarser sediment particles than for fine particles with partially cohesive characteristics. Indeed, it has been shown that fine sediments in the upper layers, tend to behave as non-cohesive (El Ganaoui et al. [26]).

Most natural cohesive sediments are heterogeneous mixtures of sand grains and cohesive particles. If the mixture contains cohesive substances it behaves as cohesive, provided it is sufficiently consolidated. Following Migniot [5], it is assumed that sediment is cohesive when the characteristic grain size reaches several tens of microns (50×10^{-6} [m]). For such conditions, the erosion threshold is greater than values that do not take into account inter-particle bonds resulting from the presence of cohesive agents (Migniot [5], Mehta [27,28], Parchure and Mehta [29]). In their studies, Sundborg [30] and Postma [31] wrote about a positive correlation between consolidation and critical shear stress. On the other hand, the research of Mitchener and Torfs [32] revealed the importance of an appropriate proportion of fine particles in mixtures of mud and sand in the initial erosion phases.

Authors of sediment logical studies on cohesive sediment transport-induced erosion were Raudkivi [33], Dade et al. [34], Mehta [35], Mehta and Lee [36]. On the other hand, for loose sands, studies were carried out by Miller et al. [37], Sleath [38], Dyer [39], Voulgaris et al. [40]. The problem of erosion of partially cohesive subsoil modified by the presence of sand was also dealt with by Merckelbach and Kranenburg [18], Le Hir et al. [41], Sanford [42], Waeles et. al. [43], and Mengual [44], among others. However, the abovementioned studies do not explain the entire erosion process resulting from the presence of granulometric ally heterogeneous mixtures containing very fine sandy and cohesive fractions in the subsoil. Alvarez-Hernandez [45] described channel experiments conducted to study the critical shear stress for erosion with increasing clay content added to sand. Van der Velden and Bijker [46] noted that the critical shear stress for erosion of natural mixed deposits with sand increased. A study by Panagiotopoulos et al. [47] using cohesive estuarine sediments mixed with quartz sand showed that as the mud content increased from 0% to 50%, the critical erosion stresses also changed. De Sutter et al. [48] published the experimental results conducted with fine sand in a circular channel. They showed the inconsistency of experimental data with existing models for constant flow conditions, both for transported layer and sediment transport in suspension (show in Figure S1 in Supplementary Material). In addition, it was noted that the flow friction velocity cannot be used as a parameter to establish an instantaneous relationship with sediment transport due to material inertia, which causes the amount of transport to reach variable values. Flemming and Delafontaine [49] and Riethmuller et al. [50] found an indirect relationship between water content and cohesive sediment fraction, which they approximated as a function of energy conservation with site-specific coefficients. Van Ledden et al. [51] conducted conceptual studies describing the transition from non-cohesive to cohesive behavior. According to them, this transition is best described by the clay content and occurs when the clay content exceeds 5–10%.

Finally, Banasiak and Verhoeven [52] show in steady sediment transport conditions the eroded partly cohesive bed produces an active granular top layer over an intact substrate, the thickness of which is up to ten times smaller than in the case of a granular bed. The cohesion of the substrate reduces the height and length of bed forms, bed form friction, and sediment transport rates.

This paper presents the experimental results carried out for the initial movement of sediment in the bottom. The experimental research was conducted in a flow test bed at the IBW PAN Gdańsk and at the laboratory of geotechnics of the Koszalin University of Technology. The primary objective was to prove that even a relatively small amount of cohesive admixtures significantly changes the dynamics, affects the magnitude of sandy sediment transport, while in terms of theoretical studies, the quantitative evaluation of such changes, based on the proposed model. In addition, an additional objective was to expand the knowledge regarding the dynamics of non-cohesive bottom-building sediments containing cohesive additives under flow conditions with a moving sediment layer at the bottom.

A series of publications by Kaczmarek et al. [53–56] addressed the development of a theoretical and numerical model for the movement of granulometric uniform sediments [55] in steady flow and heterogeneous sediments in wave motion. The mathematical tool was extensively tested for non-uniform sediments [56] using small- and large-scale laboratory data, as well as with the results of field experiments. It allowed precise determination of the vertical structure of concentration and velocity, and thus calculation of sediment transport rates for any granulometric distribution of bulk sediments, including those with a content of fine and very fine fractions in wave motion (Radosz et al. [57,58]) and in steady flows (Zawisza et al. [59]). A multilayer description of sediment flows with a full vertical structure of both concentration and velocity was used for the widest possible range of grain mobility conditions. Therefore, it seems advisable to extend this sediment transport model to the case of a mixture of sandy sediments with a low content of cohesive fractions.

The main objective of experimental studies was to collect laboratory data documenting the sediment transport rate of a mixture with small amounts of cohesive fractions in a steady flow. The experimental results were then compared with the results of present theoretical model based on the three-layer model of Kaczmarek et al. [56] for the wave motion and Zawisza et al. [59] for steady flow of granulometric ally heterogeneous sediment transport. An extension of these models was proposed here to map the inhibitory effect of cohesion forces on the sandy sediment transport. Therefore, it is possible to formulate the thesis that the presence of small amount of cohesive fractions in sediment causes an increase in the critical shear stress for the onset of sediment movement and thus a reduction in sediment velocity at the boundary between dense and contact layer above the bottom. It in turn results in a reduction in the vertical velocity and concentration profiles in both the dense layer and in the contact layer above the bottom, and consequently a reduction in the magnitude of sandy fractions transport rates. Cohesive fractions released from the bottom during transporting are then dispersed in the water and from then on do not affect the transport of sandy fractions.

2. Materials and Methods

2.1. Experimental Setup Gdańsk 2021 Measurements

In order to verify the proposed extension of a three-layer model to include a computational module for sediment transport containing cohesive fractions, a study of the effect of such fractions on the magnitude of sandy sediment transport was planned.

The experiments were carried out in a recirculating flow channel adapted to the specifics of the study on sediment transport with cohesive additives. Test station was located in the laboratory of the Institute of Hydro-Engineering of the Polish Academy of Sciences in Gdańsk (IBW PAN). Diagram of test station is shown in Figure 1.

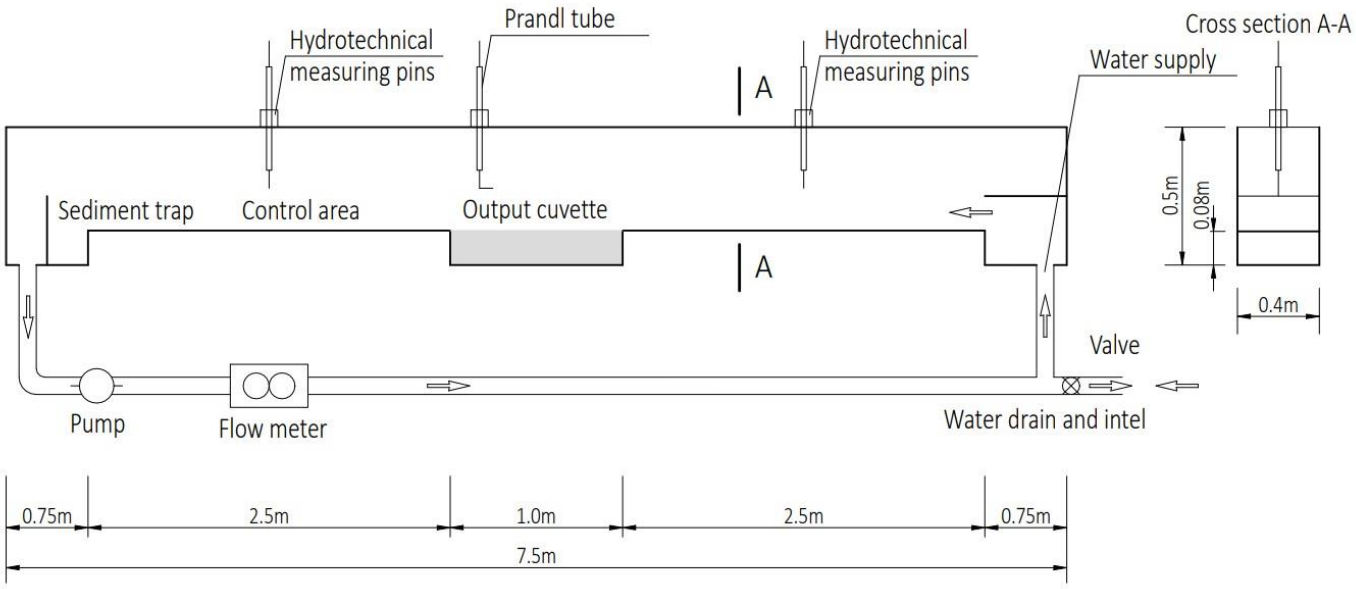

Figure 1. Experimental setup for steady flow measurements Gdańsk 2021.

Dimensions: cross-section 0.40 × 0.50 m; length 7.5 m. Both the channel and output tray and slime traps in the channel bottom made of 0.02 m thick waterproof plywood, all glued to waterproof glue with wooden dowels and all cavities filled and sanded with sandpaper and painted twice with black oil paint. The channel bottom with roughness obtained by applying a third layer of paint and spilling dry sand on it, which was later used for testing stations and making mixtures ($d_{50} = 0.23\,mm$). The channel bed slope was fixed at 0.002, with a total channel length of 750 cm divided into sections:

- Outflow section 0.73 m long with a bottom inlet—supplying the channel with water;
- The launch section is 2.50 m long;
- Tray—a cavity across the channel width with a length of 1.00 m and a height of 0.08 m;
- Test section with a length of 2.50 m;
- Sediment trap in the form of another tray—a cavity in the channel with a length of 0.73 m and a height of 0.08 m with a bottom drain—drainage of water from the channel.

Integrated channel with a pump (Grundfos: 50 Hz; Q = 137.1 m^3/h) with a system of closed water supply and drainage pipes (hoses with a nominal diameter of 7.5 cm) in a closed system and a set of control (Danfoss) and measurement apparatus (a set of Siemens flow meters with an accuracy of 0.25% of the measurement). The flow meter number 1 of the set was used in the study. An inverter was used to control the pump over the entire range.

To measure the amount of sediment in the contact layer, a set of two pipes (bottom and top) placed in the centreline of channel were used, connected by hoses with silicon pumps and collecting the water mixture into two separate plastic containers of 10 L each. The basic parameters of experiments in the flow channel of IBW PAN Gdańsk 2021 are shown in Table 1.

Table 1. Basic data from the experiment in the flow channel experiment IBW PAN Gdańsk 2021.

Parameter	Symbol	Value	Unit
Water depth	H	0.05	m
Test duration	T	900–3600	s
Representative diameter of bottom sediment grains	d_{50}	0.23	mm
Diameter clay addition	d_{50}	0.19	mm
Sediment density	ρ_s	2.65	g/cm^3
Liquid density	ρ_w	1.00	g/cm^3
Porosity of sediment	N_p	0.4	-

2.2. The Scope of Measurements

During the experiments, experimental data was collected to document the amount of sediment erosion. The velocity of sediment flow from the output tray to control area, the magnitude of sediment transport in the flume, and the amount of sediment retained in the trap were measured. Bathymetric changes in the tray were measured, and analyses were carried out on the granulometric compositions of sediment samples taken both in the initial area and in the trap.

As can be seen from the grain size curve prepared (Figure 2.), the input sediment forming the basis of mixtures analyzed is a sand with very large amount of fine fractions with $d_{50} = 0.21\ mm$, and the content of grains $d_i < 0.20\ mm$ was 38.51%. Granulometric characteristics of the studied initial sand and sediments taken from the traps—IBW PAN Gdańsk 2021 Experimental testing was carried out in three stages. The first involved experimental studies in the flow channel of sediments containing fine and ultra-fine fractions, while in the second, tests were conducted on sediments containing cohesive admixtures. In the third stage, the granulometric compositions of transported sediments were determined. The experimental results were then compared with the results of a theoretical analysis based on a present three-layer sediment transport model. Test results for sediment containing fine and ultra-fine fractions without cohesive additives are presented in Zawisza et al. [59].

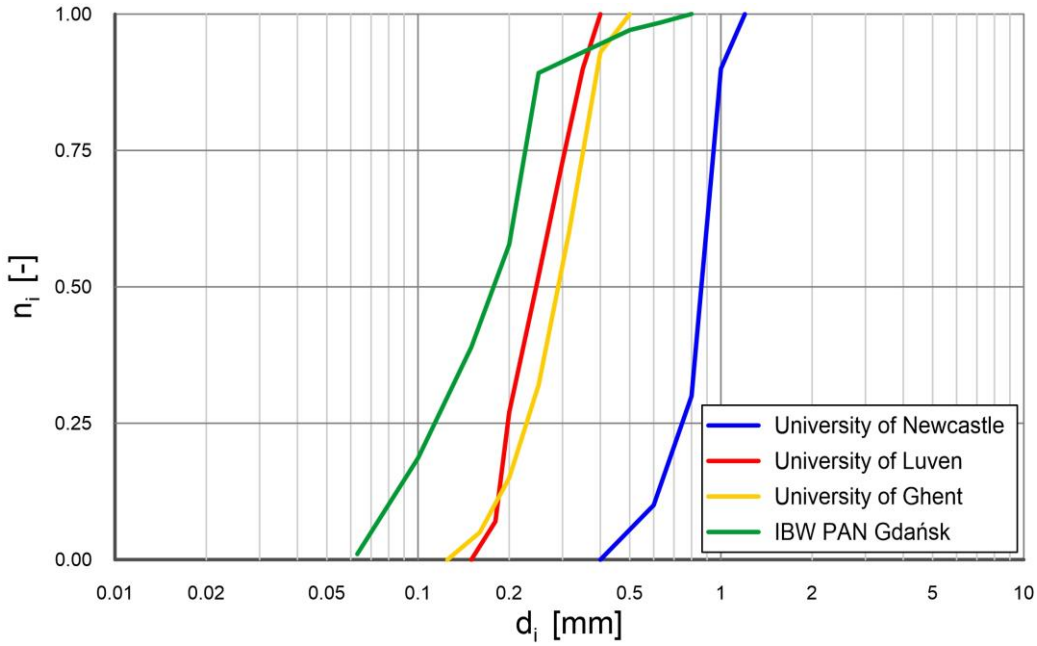

Figure 2. Grain size distributions used in experiments.

A set of hydraulic pins allowing readings with an accuracy of 0.1 mm was used for water level and bathymetry measurements. Transport velocities of suspended sand were obtained by integrating the product of velocity profiles and concentration. Laboratory experiments were carried out over a range of various flow rates from 2 to 15 L/s. During the experiments, the velocity profile was measured using a Prandtl tube. The measured vertical velocity distribution was approximated by a logarithmic profile, from which the friction velocity was determined (for details see Zawisza et al. [59).

Experiments used sand that was mechanically mixed dry in cage blender separately with the addition of clay, in different sizes, i.e., the clay accounted for 5%, 10%, 15% and 20% by weight, respectively, of the dry weight of sand forming the base of the produced mixtures used in test series. Figure 2 shows the result of sieve analysis of pure sand. As a cohesive additive, dry ground clay produced by drying and grinding natural, ecologically pure red clay, mined open-pit from the Szkucin deposit, without any additives, was used.

Preparation of the mixtures for testing followed a previously developed procedure. Calculated and weighed quantities of pure sand and dry clay were mixed in cage blender. After thorough mixing, the dry mixture was poured in layers into a plastic caste and tap water was added. The caste with prepared mixture with added clay was set aside for 24 h. After this time, excess water was floated to the surface. In the output tray of a test stand, the moist mixture was laid with light compaction.

The duration of each test was 3600 s, and 1800 s after the start of test, silicon pumps were activated for 600 s to catch suspended sediment. At the end of test, the trough was emptied of water, the condition of trays was documented by photographing, bathymetric measurements of the output tray were taken, and sediment deposited on the outfall plate and end trap was selected. The transported sediment was weighed and samples were taken into labelled containers for sieve analysis. The captured suspended sediment was also placed in containers.

Before the start of each test, samples were taken from a container filled with sediment prepared for testing, while after each test a second sample was taken, this time from the trap. The collected samples were subjected to granulometric analysis at the geotechnical laboratory of Koszalin University of Technology. Measurements were conducted using the "dry" method for all collected sediment samples with Mikro LAB sieve shaker (model: LPzE-2e, MULTISERW-Morek, Marcyporęba, Poland). Prior to the test, the samples were

dried at 1000 C for 24 h. The granulometric characteristics of the input sand under as well as the sediments taken from the catcher and control area are shown in Table 2. while the chemical and mineral compositions of cohesive admixtures are shown in Tables 3 and 4, respectively.

Table 2. Granulometric characteristics of the studied initial sand and sediments taken from the traps—IBW PAN Gdańsk 2021.

Type of Sediment	$d_{90}/d_{50}/d_{10}$
Input sand	0.23/0.22/0.14
Trap deposits	-
TR_10_13	0.25/0.22/0.13
TR_15_11	0.43/0.24/0.13
TR_15_12	0.41/0.23/0.12
TR_15_13	0.40/0.23/0.12
TR_15_14	0.42/0.23/0.13
TR_20_12	0.44/0.24/0.13
TR_20_13	0.48/0.25/0.13
TR_20_15	0.41/0.23/0.12

Table 3. Cohesive additive parameters. Chemical composition.

Chemical Compound	Content
- SiO_2	55.00–62.14%
- Al_2O_3	15.70–17.70%
- TiO_2	0.70–0.90%
- Fe_2O_3	6.09–7.90%
- MnO	0.04–0.17%
- MgO	2.20–3.20%
- CaO	0.33–1.81%
- Na_2O	0.06–0.26%
- K_2O	2.90–3.50%
- P_2O_5	0.05–0.18%
- roasting losses	7.04–13.40%

Table 4. Cohesive additive parameters. Mineral composition.

Mineral	Content
- quartz	17–25%
- kaolinite	3–10%
- illit	3–10%
- hematite	3–5%
- plagioklaz	<3%
- potassium feldspar	<3%
- goethyt	<2%
- anatase	<5%
- mixed packet minerals (vermiculite/chlorite, smectite/illite)	32–53%
- amorphous phase	15%

The results of measurements of the transport intensity of sand fractions with cohesive admixtures obtained in Gdańsk 2021 experiment are presented in Figure 3. The measured transport results are presented as a function of the measured shear velocity u'_{f*}. Additionally, the approximation of mean values of repeated tests by curve with a coefficient of determination is shown. The influence of cohesion on the measurement results is clearly

visible, because the same value of transport of sand fractions can be obtained for other values of shear stresses $\tau'_* = \rho {u'_{f*}}^2$ depending on the content of cohesive fractions in sandy sediments. The greater the content of these fractions, i.e., the greater the percentage of clay content, the greater the resistance to movement and shear stresses. This means that in order to transport the same amount of sand fractions, the flow is the greater, the greater the content of cohesive fractions in the sandy sediments. The influence of cohesion on the value of shear velocity u'_{f*} can be assessed on the basis of measurements by estimating the difference of these values u'_{f*c} for sediments with and without cohesive admixtures (Figure 3). This difference is easiest to assess for the situation when transport $q = 0$, although due to the difficulties in clearly defining the measurement situation $q = 0$, this value should be sought between the minimum measured value for $q = 0$ and the smallest measured value for $q \neq 0$ (Figure 3).

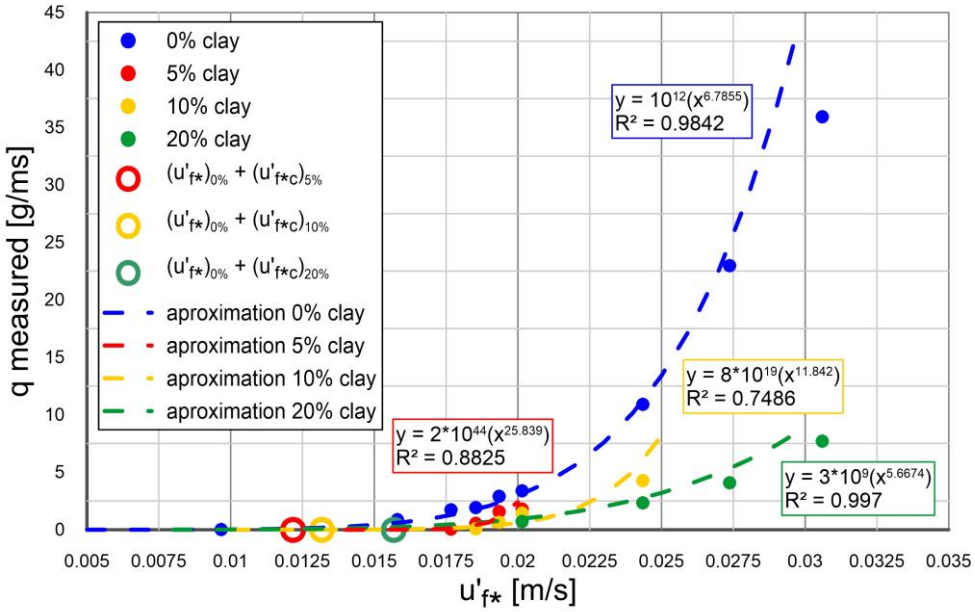

Figure 3. Results of transport rate measurements of sand fractions of sediments with cohesive admixtures obtained in Gdańsk 2021 experiment with the approximations of mean values of repeated tests by curves with a coefficients of determination.

In conclusion, the presented approach is applicable if experimentally measured shear velocity u'_{f*} and corresponding evaluation of u'_{f*c} are available. The evaluation of u'_{f*c} is relatively simple as can be seen in Figure 4, where the results of measurements of the transport intensity of sandy fractions q (g/ms) of sediments with cohesive admixtures obtained in the experiment of De Sutter et al. [48] are depicted. The measured transport results q are plotted as a function of the measured shear velocities u'_{f*}. Figure 4 shows the differences of the measured shear velocity values u'_{f*} for sediments with and without cohesive impurities. As in the case of Gdańsk 2021 experiment (Figure 3), the value u'_{f*c} for different clay contents was estimated as a value between the minimum measured value of u'_{f*} for $q = 0$ and the smallest measured value for $q \neq 0$ (Figure 4). It should be noted that cohesive stress value τ_{coh} may be evaluated based on u'_{f*c} in a following way:

$$\tau_{coh} = \tau'_* - (\tau'_*)_{ef.} = \rho\left(u'_{f*}\right)^2 - q\left(u'_{f*}\right)^2_{ef.} \quad (1)$$

where u'_{f*} is the skin shear velocity equal to $u'_{f*} = \sqrt{\frac{\tau'_*}{\rho}}$ (Figure 5b), while the effective shear velocity $\left(u'_{f*}\right)_{ef.}$ is equal to the value $\left(u'_{f*}\right)_{ef.} = u'_{f*} - u'_{f*c}$, and the shear velocity u'_{f*c} is due to cohesion. The stress value τ_{coh} is not measured here. This is precisely the

challenge that the future works must face with comparison between measurements and calculations by means of Equation (1).

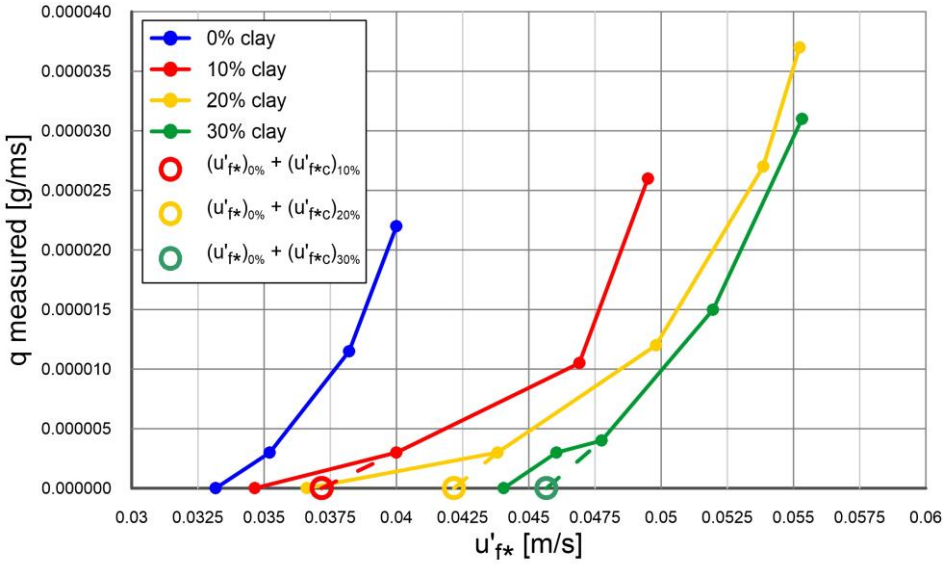

Figure 4. Transport of sand fractions in the experiments by De Sutter et al. [48].

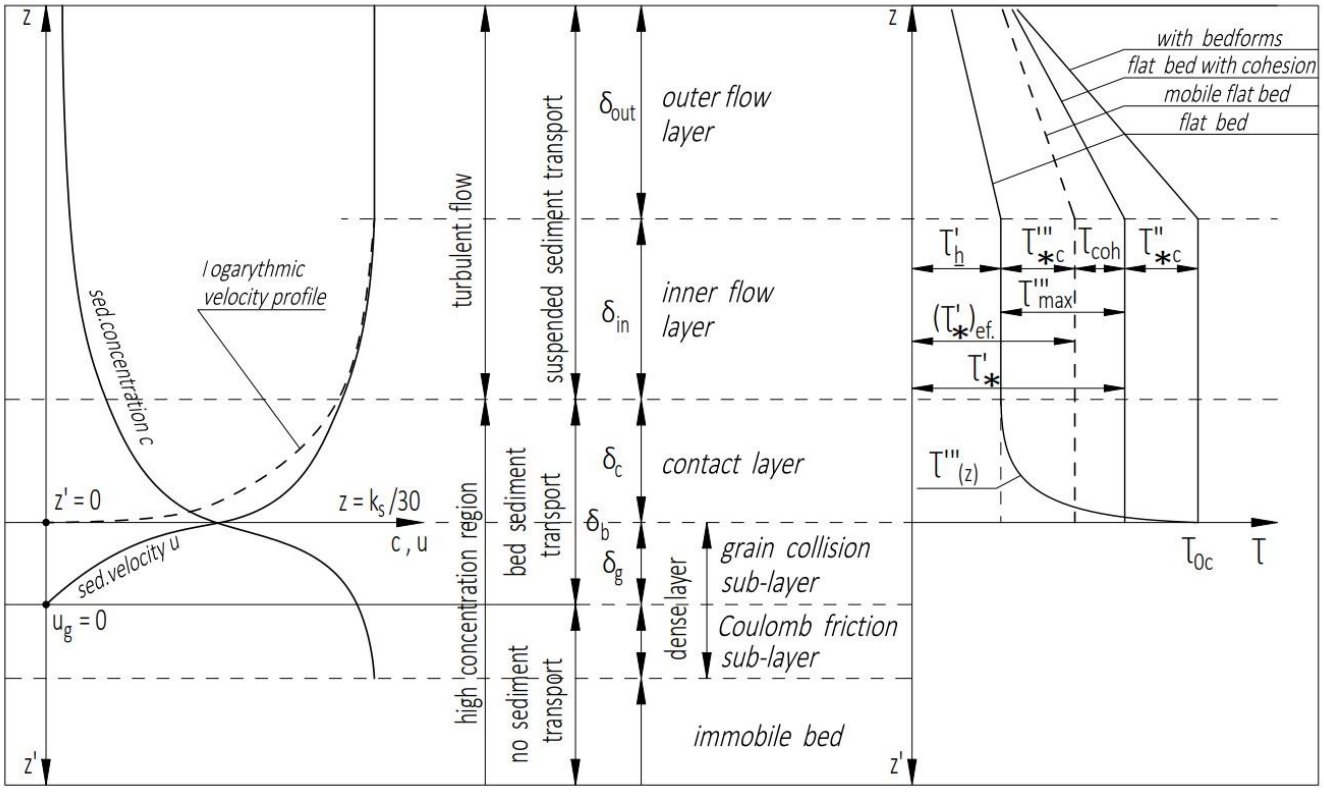

Figure 5. Vertical structure of: (**a**) sediment transport profile with velocity and concentration of the i-th fraction of sediment; (**b**) shear stress profile with cohesion stress τ_{coh}.

2.3. Theoretical Model

2.3.1. Basic Equations

The present approach is derived to modelling of transport of heterogeneous sediments, while admitting small admixture of cohesive fraction. It is assumed that cohesive part is limited by the porosity of the soil. Moreover, cohesion suppresses the transport of heterogeneous non-cohesive sediments due to an increase of critical stresses, while delaying initiation of grain motion. It is then followed by the release of cohesive content from the bottom and its spread in the whole region of the flow. In the presented model, the contribution of cohesive fractions to the net transport of sediments is neglected.

The multilayer approach for non-cohesive sediment fractions is proposed here for steady flow conditions with the specification of layers up to water surface elevation as in Figure 5: a dense layer with immobile Coulomb friction sublayer and upper dense mobile sublayer dominated by grain collisions, a contact layer, where particle collisions and turbulent lift cooperate in momentum exchange as well as a suspended sediment zone, which is divided into inner and outer flow regions. The inner flow region is characterized by a logarithmic velocity profile. Transport of sediment characterized by very high concentration takes place at the entire layer of the dense mixture, in the form of a grain flow with a specific velocity $u_g(z')$ and concentration $c_g(z')$ profile. Since both water and grains move in the mobile dense layer as well as in the layer of suspended sediment, there must be a transitional zone between these two regions, in which both velocity $u_i(z)$ and concentration $c_i(z)$ profiles of each fraction of the sediment mixture (Figure 5a) and the shear stress profile (Figure 5b) represent continuous shape. This transition zone is called the contact layer after (Kaczmarek et al. [53–56], and Zawisza et al. [59]).

The detailed description of the interaction between the soil and liquid phases was carried out by Kaczmarek et al. [55] for uniform non-cohesive sediments in steady flow and by Kaczmarek et al. [56] for non-uniform non-cohesive sediments in the wave-induced flow conditions. Hence, these models are derived to analyse two distinctive subdomains of high and low concentration separately, while including the interaction between them and employing different constitutive equations. In some models (see e. g. Longo et al. [60]) a two-phase description is proposed enforcing approximations and inevitable limitations due to application of the closure of turbulence and interactions between the sediments and the fluid body.

The present model assumes, that the presence of cohesive fractions in sediment causes an increase in the critical shear stress for the incipient sediment motion. Then, those fractions are released from the bottom and dispersed in the water. From then on, they do not affect the transport of sandy fractions. Thus, a reduction in sediment velocity at the boundary between grain collision sublayer and contact layer (Figure 5a) results in reduction in both the vertical velocity $u_g(z')$ and concentration $c_g(z')$ profiles as well as $u_i(z)$ and $c_i(z)$ vertical profiles. Then, in the moving layer of densely concentrated sediments, all sand fractions move at the velocity equal to the velocity of the mixture (at specified elevation). Hence, the interactions between the sediment fractions are assumed so strong, that the finer fractions are slowed down by the thicker ones and all the fractions are characterized by the same velocity $u_g(z')$ and concentration $c_g(z')$ vertical profiles. The model also takes into account, that the most intensive sorting of sand fractions occurs in the grain scattering process in the contact layer and in turbulent flow region, which brings those fractions into suspension. In the contact layer, vertical profiles of velocities $u_i(z)$ and concentrations $c_i(z)$ vary for individual fractions, due to turbulent fluid pulsations and chaotic collisions of grains.

The concept of shear stress variation has been proposed originally by Kaczmarek et al. [55]. Shear stress increases from the skin stress value τ_b' above the bed (Figure 5b) to the maximum value τ_0 at the bed, and then, the viscous part of this stress decays in the bed. The shear stress $\tau_*' = \rho u_{f*}'^2$ above the bed, at the top of the contact layer, is identified as an input data with the value obtained from experiments. When the cohesive fractions

are present the shear stress τ_0 at the top of the dense layer is reduced to τ_{0c}. Then, the shear stress τ'_* is the sum of bed skin friction τ'_b and drag friction τ'''_* due to motion of sediment particles, and cohesion friction τ_{coh} due to the presence of cohesion fractions while τ''_{*c} is the friction due to bed forms, when they are present. It is worth noting the reduction of stresses from the values τ''_* to the values τ''_{*c} and τ'''_* to τ'''_{*c} in the case of the presence of cohesive admixtures in sandy bed.

Profiles of the velocity $u_g(z')$ and concentration $c_g(z')$ in the dense layer are calculated using the Equations (2) and (3) in a system of coordinates with the vertical axis z' directed downwards (Figure 5a):

$$\alpha^0 \left(\frac{c_g - c_0}{c_m - c_g}\right) sin\,\varphi\, sin\, 2\,\psi + \mu_1 \left(\frac{du_g}{dz'}\right)^2 = \tau_{0c}, \tag{2}$$

$$\alpha^0 \left(\frac{c_g - c_0}{c_m - c_g}\right) (1 - sin\,\varphi\, cos\, 2\,\psi) + \mu_2 \left(\frac{du_g}{dz'}\right)^2 = \left(\frac{\mu_2}{\mu_1}\right)\Big|_{c_g = c_0} \tau_{0c} + (\rho_s - \rho)\, g \int_0^{z'} c_g dz', \tag{3}$$

where $\tau_{0c} = \rho u_{f0c}^2$; u_{f0c} is the friction velocity at the top of the dense layer; $\alpha^o = constant = \rho_s g d_r$; ρ_s is the density of sediments; g is the acceleration of gravity and ρ is water density; $c_m = 0.53$ is the maximum concentration of the bed sediment; $c_D = 0.32$ is the concentration of sand mixture at the upper limit of the dense layer; $\varphi = 24.4°$ is the quasi-static angle of internal friction; $\psi =$ angle between the major principal stress and the horizontal axis:

$$\psi = \frac{\pi}{4} - \frac{\varphi}{2}, \tag{4}$$

$\mu_1, \mu_2 =$ functions of concentration, described (after Kaczmarek et al. [53,54]) as

$$\mu_1 = \frac{0.03}{(c_m - c_g)^{1.5}} \rho_s d_r^2 \text{ and } \mu_2 = \frac{0.02}{(c_m - c_g)^{1.75}} \rho_s d_r^2. \tag{5}$$

where d_r is the representative diameter for sand mixture in the dense layer which is assumed as $d_r = d_{50}$, where d_{50} is median diameter of sand.

Assuming that settling of sediment balances the vertical exchange and the momentum exchange balances the shear stress, following Deigaard [61], Kaczmarek et al. [56] and Zawisza et al. [59] a set of two differential equations is proposed to calculate the concentration and velocity profiles of the *i*-th sediment fraction in the contact layer:

$$\left[\frac{3}{2}\left(\alpha_s \frac{d_i}{w_s}\frac{du_i}{dz}\frac{3}{2}\frac{s + c_M}{c_D} + \beta_i\right)^2 d_i^2 c_i^2 (s + c_m) + l^2\right]\left(\frac{du_i}{dz}\right)^2 = u'^2_{f*}, \tag{6}$$

$$\left[3\left(\alpha_s \frac{d_i}{w_{si}}\frac{du_i}{dz}\frac{2}{3}\frac{s + c_M}{c_D} + \beta_i\right)^2 d_i^2 \frac{du_i}{dz} c_i + l^2 \frac{du_i}{dz}\right]\frac{dc_i}{dz} = -w_{si} c_i, \tag{7}$$

where d_i is the diameter of the *i*-th sand fraction; $w_{si} =$ settling velocity of the *i*-th fraction; $c_M =$ added hydrodynamic mass coefficient; $c_D = 1.0$ is a drag coefficient; $l =$ mixing length equal to κz ; $\kappa =$ von Karman's constant, which is around 0.40; $s = \rho_s/\rho$; $(s + c_m)$ is assumed to be around value of 3.0. Coefficients $\alpha_i = \beta_i$ are calculated by the procedure which assumes the equality of the calculated sand velocity $u_i(z)$ and the logarithmic flow velocity at the water surface elevation.

Numerical solution of these equations is described in detail by Kaczmarek et al. [55] for uniform sediments in steady flow and Kaczmarek et al. [56] for non-uniform sediments in the wave motion. The set of Equations (2) and (3) as well as Equations (6) and (7) are solved using numerical integration. The boundary conditions for set of Equations (6) and (7) are values that come from calculations in the dense layer with Equations (2) and (3) i.e., the velocity of sediment $u_g(z' = 0) = u_0$ corresponds to the concentration $c_0 = 0.32$. The shear stress velocities u'_{f*} are identified as an input data with the values obtained from experiments. Finally transport q of non-cohesive fractions is calculated as:

$$q = \int_0^{\delta_q} u_g c_g \, dz' + \sum_{i=1}^{N} n_i \int_{\frac{2.5d_{50}}{30}}^{h} u_i c_i \, dz, \tag{8}$$

where h is the water depth.

Following the idea by Kaczmarek et al. [55], the mobile-bed effect parameter γ_{0c} is introduced:

$$\gamma_{0c} = \sqrt{\frac{\tau_{0c}}{\tau'_*}} = \frac{u_{f0c}}{u'_{f*}}, \tag{9}$$

In order to find the parameter γ_{0c}, it is assumed that bed sediment transport calculated for both the dense and the contact layers (Figure 5) can be compared with a semi-empirical formula by Meyer-Peter and Müller [62] (abbreviated to "MPM" below). Hence, according to the flow description shown in Figure 5, the following relationship can be postulated:

$$q_g\left(\rho\gamma_{0c}^2 u_{f*}'^2\right) + q_c\left(\rho u_{f*}'^2\right) = \Phi_{MPM}\sqrt{(s-1)g d_r^3}, \tag{10}$$

where sediment transport rate q_g in the grain collision sublayer (calculated by Equations (2) and (3)) is a function of shear stress $\rho\gamma_{0c}^2 u_{f*}'^2$.

$$q_g = \int_0^{\delta_q} u_g c_g \, dz', \tag{11}$$

while sediment transport rate q_c in the contact layer calculated by Equations (6) and (7)

$$q_c = \sum_{i=1}^{n} n_i \int_{\frac{2.5d_{50}}{30}}^{\delta_c} u_i c_i \, dz, \tag{12}$$

is a function of shear stress $\rho u_{f*}'^2$ and:

$$\Phi_{MPM} = 8\left[(\Theta'_*)_{ef.} - \Theta_c\right]^{1.5}. \tag{13}$$

$$(\Theta'_*)_{ef.} = \frac{\left(u'_{f*}\right)_{ef.}^2}{g(s-1)d_r}. \tag{14}$$

The parameter defined in Equation (14) is called the Shields parameter, while the critical Shields parameter Θ_c is a constant of the order of 0.05 for sand placed smoothly on a horizontal bed.

The flow charts of numerical algorithms for calculations of sediment transport and the mobile-bed effect parameter γ_{0c} are shown in Figure 6.

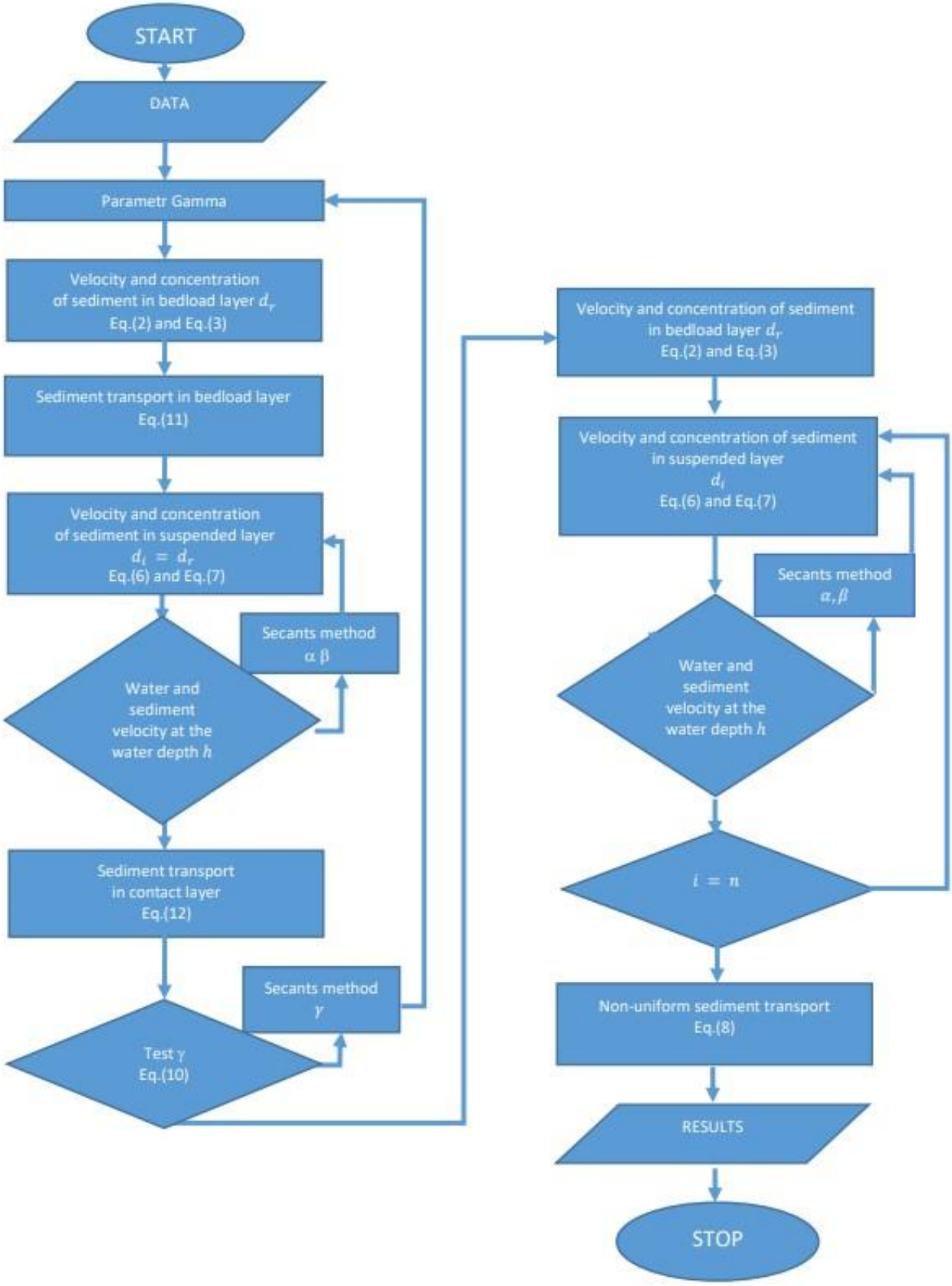

Figure 6. Flow charts of numerical algorithms for calculations of sediment transport and the mobile-bed effect parameter γ_{0c}.

2.3.2. The Influence of Cohesion on Sand Transport

Calculation results of the parameter γ_{0c} depending on the content of clay in the sandy deposit for the data of De Sutter et al. [48] are shown in Figure 7. It is worth noting that the same value in the ascending phase of the graph γ_{0c} is obtained for different percentages of clay, but in the case of sand with 0% clay content, this value is obtained for the smallest value of dimensionless friction θ'_*. The higher the clay content in the sandy deposit, the same values of the γ_{0c} parameter in the ascending phase of the curves in the graph are obtained for higher values of θ'_*. The increase in the value of θ'_* with the increase in the clay content is obviously dictated by the increase in the resistance to motion along with the increasing content of cohesive fractions.

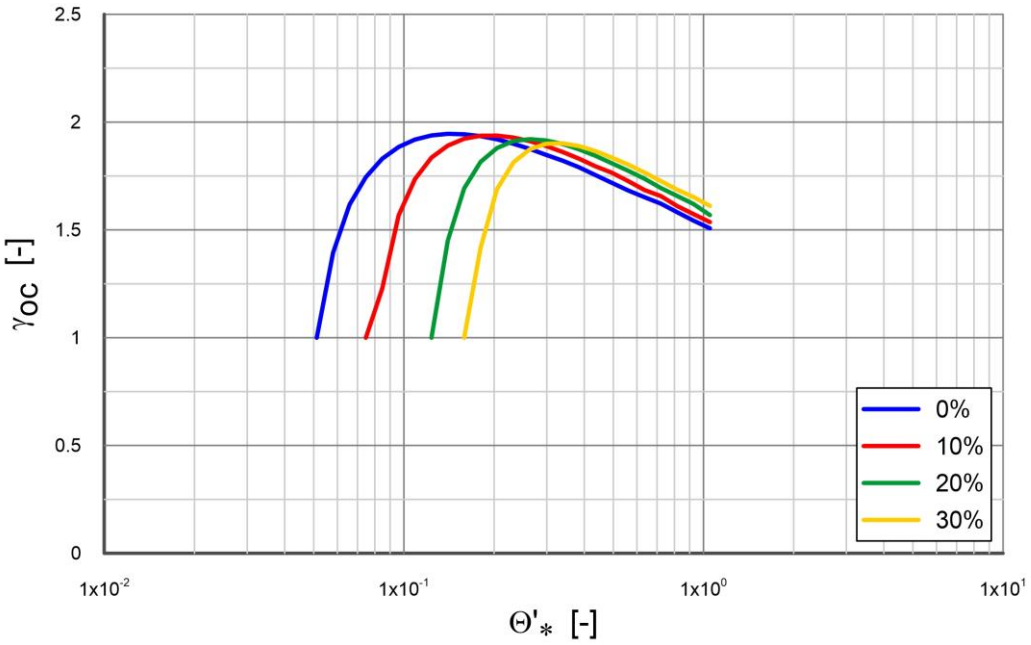

Figure 7. Influence of cohesive forces on calculations of the parameter γ_{0c} depending on the content of clay in the sandy deposit data: u'_{f*}, u'_{f*c} and $d_r = d_{50} = 0.32$ mm from the experiment of De Sutter et al. [48].

The effect of cohesion on the velocity profiles in both the contact layer and the dense layer is shown in Figure 8a,b. The data u'_{f*} and u'_{f*c} from the experiment of De Sutter et al. [48] were used in the calculations, where the calculations in the contact layer were made for diameter $d_i = 0.32\,mm$, and in the dense layer for $d_r = d_{50} = 0.32\,mm$. It can be seen that the cohesion causes a decrease in the velocities at the interface of the contact layer of the dense layer, which in turn causes a decrease in the vertical velocity profiles in both the contact layer and the dense layer. The effect of cohesion on the vertical concentration profiles in the contact layer and in the dense layer is shown in Figure 8c,d. It can be seen that the cohesion reduces the friction value at the interface between the contact layer and the dense layer from τ_0 to τ_{0c} (Figure 5b) and, as a result, reduces the vertical concentration profiles inside the dense layer according to the system of Equations (2) and (3). The reduced value of the velocity at the separation boundary of the above-mentioned layers results in a reduction of the vertical concentration profile inside the contact layer and above, according to the system of Equations (4) and (5).

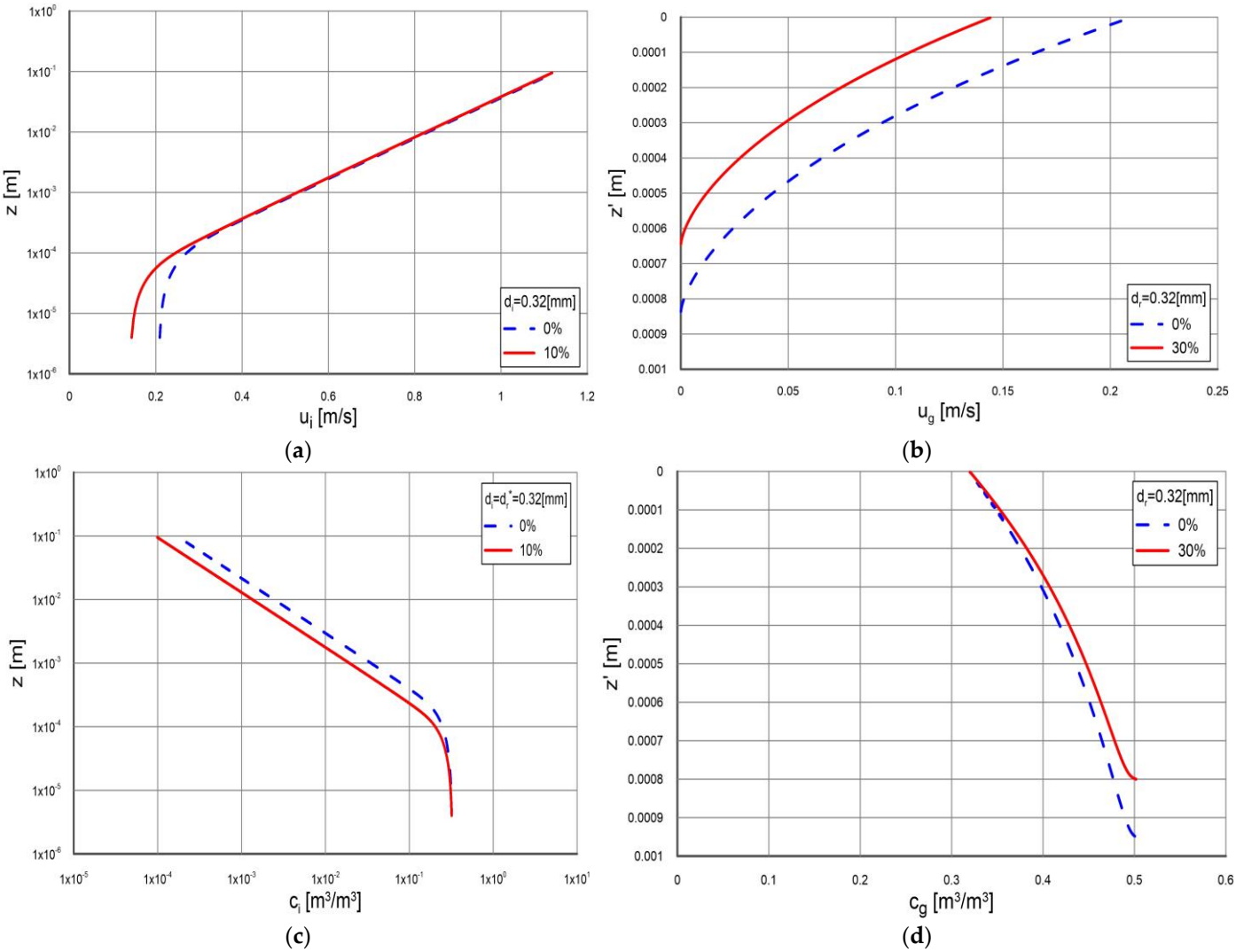

Figure 8. Influence of cohesive forces of calculations of velocity profiles in: (**a**) contact layer; (**b**) in dense layer and concentration profiles in: (**c**) contact layer, (**d**) in dense layer; data: u'_{f*} and u'_{f*c} from the experiment of De Sutter et al. [48].

The impact of not taking cohesive forces into account on the transport of sand fractions is shown in Figure 9, where the results of calculations of the transport intensity of sand fractions are presented in the case when the bottom is made of sandy sediments with cohesive admixtures and when there are no such admixtures. Transport calculations were carried out using Equations (1)–(14), but without taking cohesion into account, i.e., assuming $\tau_{coh} = 0$, $\gamma_{0c} = \gamma_0$, $u'_{f*c} = 0$, $\tau_0 = \tau_{0c}$ and $\tau'_* = (\tau'_*)_{ef.}$. With such assumptions, when the bottom is composed of sandy sediments with cohesive admixtures, the results are significantly overestimated in relation to the measurement results. Thus, not taking cohesive forces into account in the calculations may lead to significant differences between the results of calculations and measurements.

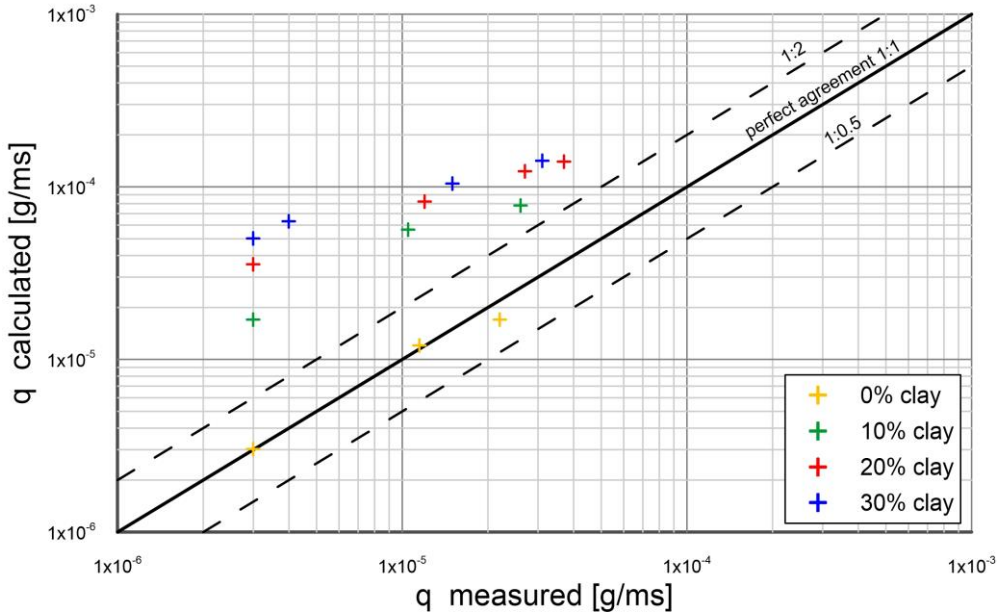

Figure 9. Influence of disregarding cohesion on transport rate calculations for De Sutter [48].

3. Comparison of Calculations with Measurements

Comparison of transport calculations of sand fractions from the sandy substrate with cohesive admixtures with the results of measurements carried out during Gdańsk 2021 experiment is shown in Figure 10. Transport calculations were carried out using Equations (1) ÷ (14) taking into account cohesion, i.e., with the measured quantities u'_{f*} and u'_{f*c} as input quantities. The results were consistent within plus/minus a coefficient of two. In turn, the agreement of the results is much worse for the results of transport calculations using Equations (1) ÷ (14), but without taking into account cohesion, i.e., for $u'_{f*c} = 0$. In this case, the calculation results significantly exceed the measurement results. In addition, Figure 10 shows the results of transport calculations of sand fractions without taking cohesion into account, but taking into account the effects recently described by Zawisza et al. [59] concerning the probable deficit in the availability of very fine fractions in the substrate.

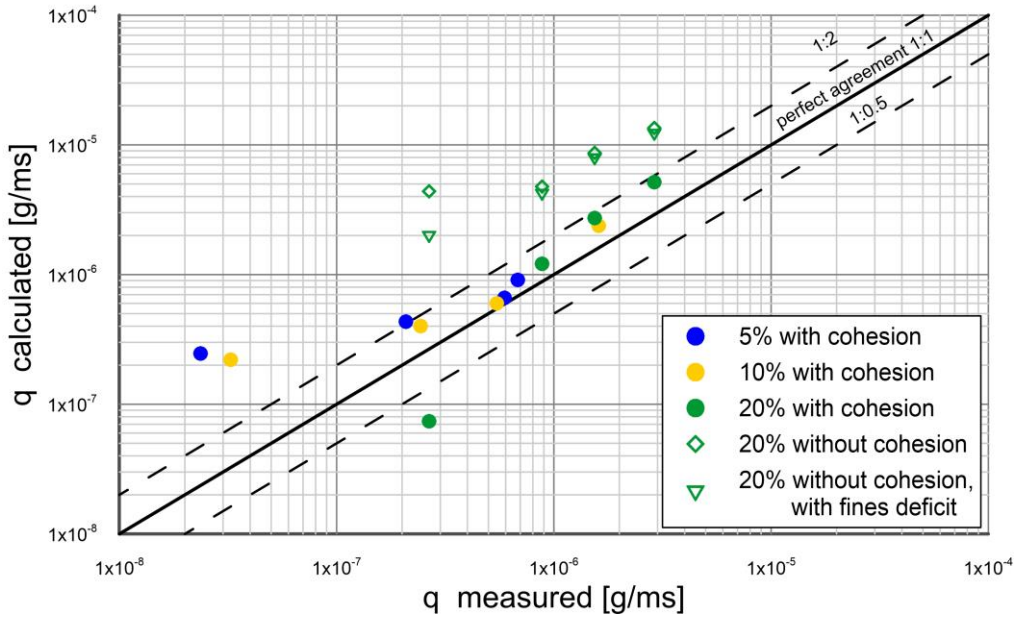

Figure 10. Comparison of sand transport calculations with Gdańsk 2021 measurements.

Figure 11 presents comparison of sand transport calculations with Gdańsk 2021 measurements with the approximation of mean values of repeated tests by linear curve with a coefficient of determination. Agreement was obtained within plus/minus a coefficient of two of the measurements.

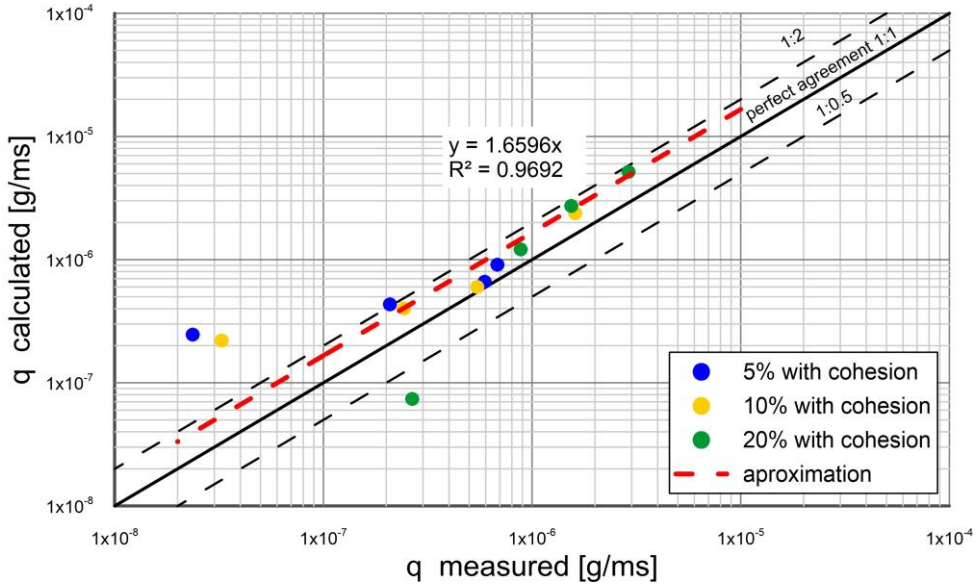

Figure 11. Comparison of sand transport calculations with Gdańsk 2021 measurements the approximation of mean values of repeated tests by linear curve with a coefficient of determination $R^2 = 0.9692$.

Figure 12 shows the results of calculations of transport of sand fractions in a substrate with different content of cohesive fractions in comparison with the results of measurements made by De Sutter et al. [48] with the approximation of mean values of repeated tests by linear curve with a coefficient of determination. Agreement was obtained within plus/minus a coefficient of two of the measurements.

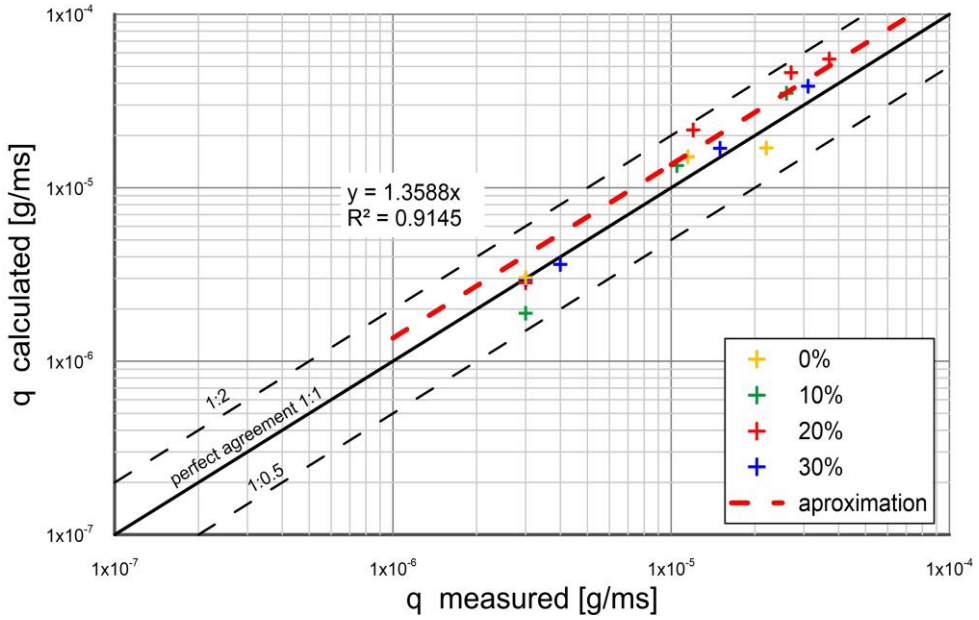

Figure 12. Comparison of sand transport calculations with measurements by De Sutter et al. [48] with the approximation of mean values of repeated tests by linear curve with a coefficient of determination $R^2 = 0.9145$.

Figures 13 and 14 show the results of comparisons of transport calculations of sand fractions in the substrate with different content of cohesive fractions with the results of measurements carried out by Torfs [63] and Alvarez-Hernandez [45], accordingly. Figures 13 and 14 present also the approximation of mean values of repeated tests by linear curve with a coefficient of determination. Again, the consistency of the calculations with the measurements was achieved within plus/minus a factor of two of the measurements. The parameters of all experiments selected for comparisons are shown in Table 5.

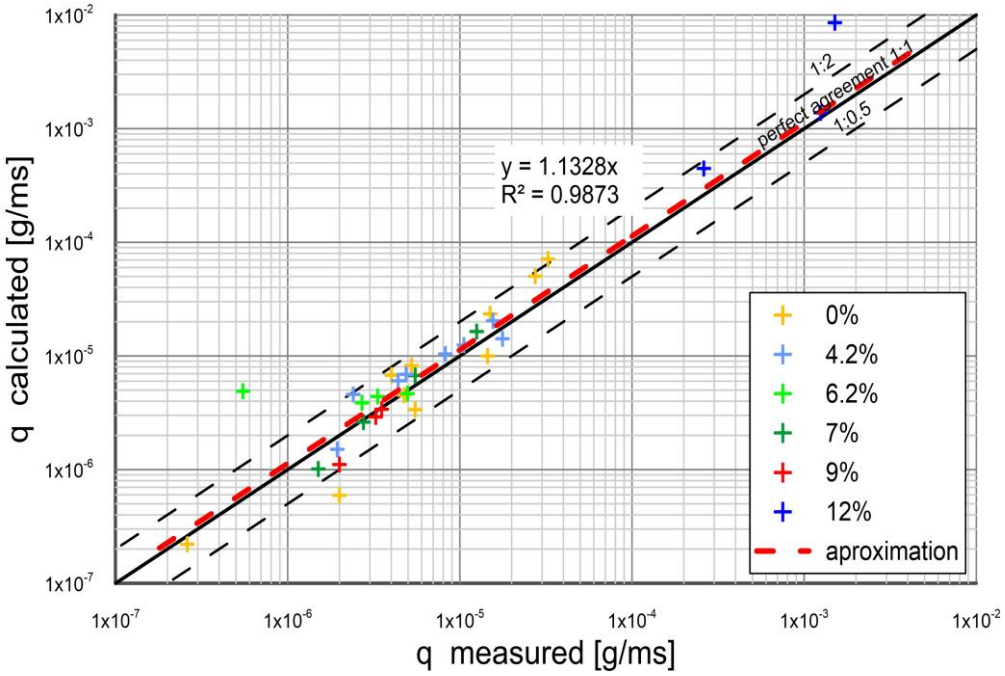

Figure 13. Comparison of sand transport calculations with measurements by Torfs [63] the approximation of mean values of repeated tests by linear curve with a coefficient of determination $R^2 = 0.9873$.

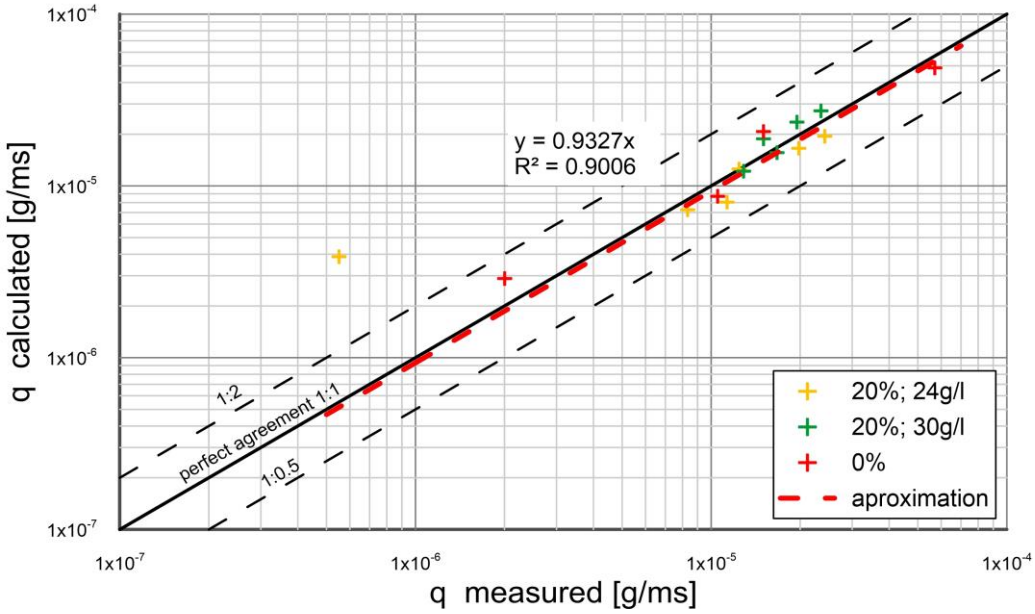

Figure 14. Comparison of sand transport calculations with measurements by Alvarez -Hernandez [45] the approximation of mean values of repeated tests by linear curve with a coefficient of determination $R^2 = 0.9006$. Addition of 20% clay with two densities c = 24 g/L and 30 g/L.

Table 5. Parameters of experiments selected for comparisons.

Experiment	h [m]	Sand d_{50}[mm]	u'_{f*} [m/s]	Additional Substance	Percentage Share of Additional Substance [%]	u'_{f*c} [m/s]
UNewcastle 1990 Alvarez-Hernandez [45]	0.081–0.310	0.90		clay gel c = 24 g/L	20	0.0025
				clay gel c = 30 g/L	20	0.0050
ULuven 1995 Torfs [63]	0.053–0.195	0.21	0.028 ÷ 0.053	montmorillonite	7	0.0075
					9	0.0900
UGhent 1998 De Sutter et al. [48]	0.081–0.095	0.32	0.033 ÷ 0.055	clay	10	0.0040
					20	0.0090
					30	0.0125
IBW PAN Gdańsk 2021	0.05	0.22	0.031 ÷ 0.097	clay	5	0.0025
					10	0.0035
					20	0.0061

4. Conclusions

Theoretical and experimental studies on transport of sediment mixtures in steady flow that were conducted in this paper allowed us to draw the following conclusions:

1. The results of experimental data were compared with the results of theoretical analysis based on the three-layer model by Kaczmarek et al. [55] for uniform sediments in steady flow, by Kaczmarek et al. [56] for non-uniform sediments in the wave motion and by Zawisza et al. [59] for non-uniform sediments in the steady flow. An extension of these models is proposed here in order to determine the inhibitory effect of cohesion admixtures on the transport of sand fractions. The present model assumes, that the presence of small amount of cohesive fractions in sediment causes an increase in the critical shear stress for the incipient sand motion and consequently a reduction in the magnitude of sand transport. Then, the cohesive fractions are released from the bottom and dispersed in the water. From then on they do not affect the transport of sand fractions.
2. In the present model the shear stress at the top of the contact layer is identified as an input data with the value obtained for experiments. This value increases depending on the content of cohesive fractions in sediment. The greater the content of these fractions, the greater the resistance to movement. The difference between the values of shear velocity for sediments with and without cohesive admixtures is also identified here as an input data with the value from experiments. This value is related with the stresses due to cohesion.
3. It can be seen from the model results the cohesion reduces the shear stress at the top of the dense layer and, as a result, reduces vertical concentration and velocity profiles of sand fractions inside the dense on contact layers. Thus, transport rate of these fractions is reduced.
4. In order to verify the proposed extension of a three layer model the experiments in the laboratory of the Institute of Hydro-Engineering of the Polish Academy of Sciences in Gdańsk were carried out. The experiments were carried out for sand alone and with cohesive admixtures in the form of clay in an amount of 5, 10, 15 and 20% by weight. The amount of sand fractions retained in the trap and along the control area was measured.
5. The experimental results were composed with the calculations by the present model. The other results from literature were also used for comparison. An agreement between transport calculations of sand fractions in a substrate with different content of cohesive fractions and the results of measurements was obtained within plus/minus a coefficient of two of the measurements.

6. The present model is applicable to non-uniform non-cohesive sediments with small amount of cohesive fractions, while assuming the maximum cohesive fraction content limited by the porosity of the soil. Moreover, at present, the modeling requires experimentally determined shear velocity. Further model development activities will comprise the measurements of stresses due to cohesion and their comparison with the present model estimations based on the shear velocity measurements.

Supplementary Materials: The following supporting information can be downloaded at: https://www.mdpi.com/article/10.3390/w15040804/s1, Figure S1: Experimental setup for steady flow measurements by De Sutter et al. [48], Figure S2. Scheme of the test stand by Torfs [63]. Legend: 1 – inflow area; 2 – measuring section (sediment); 3 – sediment siphon; 4 – outflow section; 5 – lower tank; 6- upper tank; 7 - channel tank; 8 - flow meter; 9 - solenoid valve; 10 - valves; 11 - pump; 12- load cell; 13- Prandtl tubes, Figure S3. Scheme of the test by Alvarez – Hernandez [45].

Author Contributions: Conceptualization, J.Z. and L.M.K.; methodology, J.Z., L.M.K. and J.B.; formal analysis, J.Z., L.M.K., J.B. and I.R.; investigation, J.Z., L.M.K., J.B. and I.R.; resources, L.M.K.; writing—original draft preparation, J.Z. and L.M.K.; writing—review and editing, J.Z., L.M.K. and I.R.; supervision, L.M.K.; project administration, J.Z. and L.M.K.; funding acquisition, J.Z. and L.M.K. All authors have read and agreed to the published version of the manuscript.

Funding: The research was financially supported by "ZINTEGROWANI- Kompleksowy Program Rozwoju Politechniki Koszalińskiej" nr POWR.03.05.00-00-Z055/18: Projekt współfinansowany ze środków Unii Europejskiej z Europejskiego Funduszu Społecznego w ramach Programu Operacyjnego Wiedza Edukacja Rozwój 2014-2020 and the research project of the Koszalin University of Technology Faculty of Civil Engineering, Environmental and Geodetic Sciences: Dynamika niespoistego, niejednorodnego granulometrycznie ośrodka gruntowego w przepływie stacjonarnym i ruchu falowym w warunkach silnie nachylonego dna—funds no.: 524.01.07; project manager: L.K.

Data Availability Statement: The data presented in this study are available upon request from the corresponding author.

Conflicts of Interest: The authors declare no conflict of interest.

References

1. Du Boys, M.P. Le Rhone et les Rivieres a Lit affouillable. *Ann. De Ponts Et Chausses* **1879**, *18*, 141–195.
2. Smoluchowski, M. Versucheiner Mathematischen Theorie der Koagulations kinetic Kolloidlösun-gen. *Z. Fur Phys.* **1917**, *92*, 129–168.
3. Camp, T.R.; Stein, P.C. Velocity Gradients and Internal Work in Fluid Motion. *J. Boston Soc. Civ. Eng.* **1943**, *30*, 219–237.
4. Partheniades, E. Erosion and Deposition of Cohesive Soils. *J. Hydraul. Div.* **1965**, *91*, 105–139. https://doi.org/10.1061/jyceaj.0001165.
5. Migniot, C. Etude des propriétés physiques de different sediment strès fins et de leur comportement sous des actions hydrodynamiques. *La Houille Blanche* **1968**, *7*, 591–620.
6. Ives, K.J. (Ed.) Rate theories. In *The Scientific Basic of Flocculation*; Sijthoff and Noordoff International Publishers: Alphen aan den Rijn, The Netherlands, 1978; p. 37–61.
7. Winterwerp, J.C. A simple model for turbulence induced flocculation of cohesive sediment. *J. Hydraul. Res.* **1998**, *36*, 309–326. https://doi.org/10.1080/00221689809498621.
8. Winterwerp, J.; Kranenburg, C. *Fine Sediment Dynamics in the Marine Enviroment*; Elsevier: Amsterdam, The Netherlands, 2002; ISBN 0-444-51136-9.
9. McAnally, W.H.; Mehta, A.J. Aggregation Rate of Fine Sediment. *J. Hydraul. Eng.* **2000**, *126*, 883–892. https://doi.org/10.1061/(asce)0733-9429(2000)126:12(883).
10. Tsai, C.-H.; Iacobellis, S.; Lick, W. Flocculation of Fine-Grained Lake Sediments Due to a Uniform Shear Stress. *J. Great Lakes Res.* **1987**, *13*, 135–146. https://doi.org/10.1016/s0380-1330(87)71637-2.
11. Lick, W.; Lick, J. Aggregation and Disaggregation of Fine-Grained Lake Sediments. *J. Great Lakes Res.* **1988**, *14*, 514–523. https://doi.org/10.1016/s0380-1330(88)71583-x.
12. Tsai, C.H.; Hwang, S.C. Flocculation of sediment from the Tanshui River estuary. *Mar. Freshw. Res.* **1995**, *46*, 383–392.
13. Winterwerp, J.C.; Manning, A.J.; Martens, C.; de Mulder, T.; Vanlede, J. A heuristic formula for turbulence-induced flocculation of cohesive sediment. *Estuar. Coast. Shelf Sci.* **2006**, *68*, 195-207.

14. Hawley, N. Settling velocity distribution of natural aggregates. *J. Geophys. Res. Atmos.* **1982**, *87*, 9489–9498. https://doi.org/10.1029/jc087ic12p09489.
15. Meakin, P. Fractal Aggregation. *Adv. Colloid Interface* **1988**, *28*, 249–331. http://dx.doi.org/10.1016/0001-8686(87)80016-7
16. Dyer, K.; Manning, A. Observation of the size, settling velocity and effective density of flocs, and their fractal dimensions. *J. Sea Res.* **1999**, *41*, 87–95. https://doi.org/10.1016/s1385-1101(98)00036-7.
17. Kranenburg, C. The fractal structure of cohesive sediment aggregates. *Estuar. Coast. Shelf Sci.* **1994**, *39*, 451-460.
18. Merckelbach, L.M.; Kranenburg, C. Determining effective stress and permeability equations for soft mud from simple laboratory experiments. *Géotechnique* **2004**, *54*, 581–591. https://doi.org/10.1680/geot.2004.54.9.581.
19. Khelifa, A.; Hill, P.S. Models for effective density and settling velocity of flocs. *J. Hydraul. Res.* **2006**, *44*, 390–401. https://doi.org/10.1080/00221686.2006.9521690.
20. Boyer, K.K.; Hult, G.T.M. Extending the supply chain: Integrating operations and marketing in the online grocery industry. *J. Oper. Manag.* **2005**, *23*, 642–661. https://doi.org/10.1016/j.jom.2005.01.003.
21. Winterwerp, J.C.; van Kesteren, W.G.M. Introduction to the Physics of Cohesive Sediment in the Marine Environment. In *Developments in Sedimentology*; Series no. 56; Elsevier: Amsterdam, The Netherlands, 2004; p. xiii + 466, ISBN 0-444-515534.
22. Hjulstrom, F. Studies of Morphological Activity of Rivers as Illustrated by the River Fyris. *Bull. Geol. Inst. Univ. Upps.* **1935**, *25*, 221–527.
23. Shields, A. *Application of Similarity Principles and Turbulence Research to Bed-Load Movement*; California Institute of Technology: Pasadena, CA, USA, 1936.
24. Wiberg, P.L.; Smith, J.D. Calculations of the critical shear stress for motion of uniform and heterogeneous sediments. *Water Resour. Res.* **1987**, *23*, 1471–1480. https://doi.org/10.1029/wr023i008p01471.
25. Dey, I. *Grounding Grounded Theory: Guidelines for Qualitative Inquiry*; Emerald Group Publishing Limited: Bradford, UK, 1999; p. 300.
26. El Ganaoui, O.; Schaaff, E.; Boyer, P.; Amielh, M.; Anselmet, F.; Grenz, C. The deposition and erosion of cohesive sediments determined by a multi-class model. *Estuar. Coast. Shelf Sci.* **2004**, *60*, 457–475. https://doi.org/10.1016/j.ecss.2004.02.006.
27. Mehta, A.J. Resuspension potential of cohesive sediment bed: Estuarine comparisons. In *Proceedings of the Sixth Biennal International Estuarine Research Conference*, Elsevier, New York, NY, USA, 1982; pp. 591–601.
28. Mehta, A.J. Review notes on cohesive sediment erosion. In *Proceedings of the a Specialty Conference on Quantitative Approaches to Coastal Sediment Processes*; ASCE: New York, NY, USA; 1991, pp. 40–53.
29. Parchure, T.M.; Mehta, A.J. Erosion of Soft Cohesive Sediment Deposits. *J. Hydraul. Eng.* **1985**, *111*, 1308–1326. https://doi.org/10.1061/(asce)0733-9429(1985)111:10(1308).
30. Sundborg, A. The River Klaralven. A Study of Flu- vial Processes. *Geogr. Ann.* **1956**, *38*, 238–316.
31. Postma, H. Sediment transport and sedimentation in the estuarine environment. In *American Association for Advancement of Science*; Estuaries, G.H., Ed.; Washington, DC, USA, 1967, pp. 158–179.
32. Mitchener, H.; Torfs, H. Erosion of mud/sand mixtures. *Coast. Eng.* **1996**, *29*, 1–25, DOI:10.1016/S0378-3839(96)00002-6.
33. Raudkivi, A.J.; Witte, H.H. Development of Bed Features. *J. Hydraul. Eng*. **1990**, *116*, 1063–1079, DOI: 10.1061/(ASCE)0733-9429(1990)116:9(1063).
34. Dade, W.; Nowell, A.; Jumars, P. Predicting erosion resistance of muds. *Mar. Geol.* **1992**, *105*, 285–297, DOI: 10.1016/0025-3227(92)90194-m.
35. Mehta, A.J. Nearshore and Estuarine Cohesive Sediment transport. In *Coastal and Estuarine Studies*; American Geophysical Union: Washington, DC, USA, 1993; Volume 42, 592p.
36. Mehta, A.J.; Lee, S.Ch. *Problems in Linking the Threshold Condition for the Transport of Cohesionless and Cohesive Sediment Grain*; Coastal and Oceanographic Engineering Department University of Florida Gainesville: Gainesville, FL, USA, 1994; pp. 170–177.
37. Miller, M.C.; Mccave, I.N.; Komar, P.D. Threshold of sediment motion under unidirectional currents. *Sedimentology* **1977**, *24*, 507–527, DOI: 10.1111/j.1365-3091.1977.tb00136.x.
38. Sleath, J.F.A. *Sea Bed Mechanics*; Wiley Interscience: Chichester, UK, 1984; ISBN047189091X/9780471890911.
39. Dyer, K.R. *Coastal and Estuarine Sediment Dynamics*; Wiley Interscience: Chichester, UK, 1986; 342p.
40. Voulgaris, G.; Wallbridge, S.; Tomlinson, B.N.; Collins, M.B. Laboratory investigations into wave period effects on sand bed erodibility under the combined action of waves and currents. *Coastal Eng*. **1995**, *26*, 117–134.
41. Le Hir, P.; Cann, P.; Waeles, B.; Jestin, H.; Bassoullet, P. Erodibility of natural sediments: Experiments on sand/mud mixtures from laboratory and field erosion tests. In *Sediment and Ecohydraulics*; Kusuda, T., Yamanishi, H., Spearman, J., Gailani, J., Eds.; Elsevier: Amsterdam, The Netherlands, 2008; Volume 9, pp. 137–153, DOI: 10.1016/S1568-2692(08)80013-7.
42. Sanford, L.P. Modelling a dynamically varying mixed sediment bed with erosion, deposition, bioturbation, consolidation, and armoring. *Comput. Geosci.* **2008**, *34*, 1263–1283.
43. Waeles, B.; Le Hir, P.; Lesuer, P**.** A 3D morphodynamic process-based modeling of a mixed sand/mud coastal environment: The Seine estuary, France. In *Sediment and Ecohydraulics. Proceedings in Marine Science*; Kusuda, T., Yamanishi, H., Spearman, J., Gailani, J.Z., Eds.; Elsevier: Amsterdam, The Netherlands, 2008; Volume 9, pp. 477–498.

44. Mengual, X.; Kerr, P.; Norrbom, A.L.; Barr, N.B.; Lewis, M.L.; Stapelfeldt, A.M.; Scheffer, S.J.; Woods, P.; Islam, M.-S.; Korytkowski, C.A.; et al. Phylogenetic relationships of the tribe Toxotrypanini (Diptera: Tephritidae) based on molecular characters. *Mol. Phylogenetics Evol.* **2017**, *113*, 84–112. https://doi.org/10.1016/j.ympev.2017.05.011.
45. Alvarez-Hernandez, E. The Influence of Cohesion on Sediment Movement in Channels of Circular Cross Section**.** Ph.D. Thesis, University of Newcastle upon Tyne, Newcastle upon Tyne, UK, 1990.
46. Pluim-Van der Velden, E.T..; Bijker, E.W. Locals scour near submarine pipelines on a cohesive bottom. BOSS 92, 6th Intl Conf on the Behaviour of Offshore Structures; 7–10 July 1992; London, UK; BPP Tech Services Ltd.: London, UK.
47. Panagiotopoulos, I.; Voulgaris, G.; Collins, M. The influence of clay on the threshold of movement of fine sandy beds. *Coast. Eng.* **1997**, *32*, 19–43. https://doi.org/10.1016/s0378-3839(97)00013-6.
48. De Sutter, R.; Huygens, M.; Verhoeven, R. Flume experiments of sediment transport in unsteady flow. In *Transactions on Engineering Sciences*; WIT: Cambridge, MA, USA, 1998; Volume 18, ISSN 1743-3533.
49. Flemming, B.W.; Delafontaine, M.T. Mass physical properties of muddy intertidal sediments: Some applications, misapplications and non-applications. *Cont. Shelf Res.* **2000**, *20*, 1179–1197. https://doi.org/10.1016/s0278-4343(00)00018-2.
50. Riethmuller, R.; Heineke, M.; Kuhl, H.; Keuker-Rudiger, R. Chlorophyll a concentration as an index of sediment surface stabilization of microphyto—benthos. *Cont. Shelf Res.* **2000**, *20*, 1351–1372.
51. Van Ledden, M.; van Kesteren, W.; Winterwerp, J. A conceptual framework for the erosion behaviour of sand–mud mixtures. *Cont. Shelf Res.* **2004**, *24*, 1–11. https://doi.org/10.1016/j.csr.2003.09.002.
52. Banasiak, R.; Verhoeven, R. Transport of Sand and Partly Cohesive Sediments in a Circular Pipe Run Partially Full. *J. Hydraul. Eng.* **2008**, *134*, 216–224. https://doi.org/10.1061/(asce)0733-9429(2008)134:2(216).
53. Kaczmarek, L.M.; Sawczyński, S.; Biegowski, J. Hydrodynamic Equilibrium for Sediment Transport and Bed Response to Wave Motion. *Acta Geophys.* **2015**, *63*, 486–513. https://doi.org/10.1515/acgeo-2015-0008.
54. Kaczmarek, L.M.; Sawczyński, S.; Biegowski, J. An Equilibrium Transport Formula for Modeling Sedimentation of Dredged Channels. *Coast. Eng. J.* **2017**, *59*, 1750015-1–1750015-35. https://doi.org/10.1142/s0578563417500152.
55. Kaczmarek, L.M.; Biegowski, J.; Sobczak, Ł. Modeling of Sediment Transport in Steady Flow over Mobile Granular Bed. *J. Hydraul. Eng.* **2019**, *145*. https://doi.org/10.1061/(ASCE)HY.1943-7900.0001566.
56. Kaczmarek, L.M.; Biegowski, J.; Sobczak, Ł. Modeling of Sediment Transport with a Mobile Mixed-Sand Bed in Wave Motion. *J. Hydraul. Eng.* **2022**, *148*, 04021054. https://doi.org/10.1061/(ASCE)HY.1943-7900.0001957.
57. Radosz, I.; Zawisza, J.; Biegowski, J.; Paprota, M.; Majewski, D.; Kaczmarek, L.M. An Experimental Study on Progressive and Reverse Fluxes of Sediments with Fine Fractions in Wave Motion. *Water* **2022**, *14*, 2397. https://doi.org/10.3390/w14152397.
58. Radosz, I.; Zawisza, J.; Biegowski, J.; Paprota, M.; Majewski, D.; Kaczmarek, L.M. An Experimental Study on Progressive and Reverse Fluxes of Sediments with Fine Fractions in the Wave Motion over Sloped Bed. *Water* **2023**, *15*, 125. https://doi.org/10.3390/w15010125.
59. Zawisza, J.; Radosz, I.; Biegowski, J.; Kaczmarek, L.M. Transport of sediment mixtures in steady flow with an extra contribution of their finest fractions. Laboratory tests and modelling. *Water* 2023, in press.
60. Longo, S. Two-Phase Flow Modeling of Sediment Motion in Sheet-Flows above Plane Beds. *J. Hydraul. Eng.* **2005**, *131*, 366–379. https://doi.org/10.1061/(asce)0733-9429(2005)131:5(366).
61. Deigaard, R. A note on the three-dimensional shear stress distribution in a surf zone. *Coast. Eng.* **1993**, *20*, 157–171. https://doi.org/10.1016/0378-3839(93)90059-h.
62. Meyer-Peter, E.; Müller, R. Formulas for bed-load transport. In Proceedings of the 2nd Meeting of the International Association for Hydraulic Structures Research, Delft, The Netherlands, 7 June 1948, pp. 39–64.
63. Torfs, H. Erosion of mud/sand mixtures. Ph.D. Thesis,. Leuven, Belgium, October 1995.